RSC Advances

PAPER

View Article Online
View Journal | View Issue

Cite this: *RSC Adv.*, 2021, **11**, 21343

The photophysical properties of naphthalene bridged disilanes†

Vipin B. Kumar,[ab] Cassandra L. Fleming,[c] Sai Shruthi Murali,[d] Paul A. Hume,[bd] Nathaniel J. L. K. Davis,[bd] Tilo Söhnel[ab] and Erin M. Leitao[*ab]

Received 16th April 2021
Accepted 8th June 2021

DOI: 10.1039/d1ra02961d

rsc.li/rsc-advances

Structural isomers of naphthalene-bridged disilanes were prepared *via* catalytic intramolecular dehydrocoupling of disilyl precursors using Wilkinson's catalyst. Interestingly, it was observed that interchanging the side groups on the silicon atoms altered the photophysical properties of the bridged disilanes. Herein, we report the first example of naphthalene bridged disilanes forming excimers in non-polar solvents. Cyclic voltammetry experiments and DFT calculations were performed to analyse the band gaps of the compounds and σ–π mixing in the bridged disilanes.

Introduction

The unique sigma electron delocalisation (σ-conjugation) present across catenated Si atoms grants polysilanes useful properties, such as absorption in the UV region and semi-conducting capability, when compared to the analogous carbon-based polymers.[1–3] This feature is attributed to the fact that silicon has a lower ionization energy and a higher electron affinity compared to carbon, resulting in a lower singlet $\sigma_{sisi} - \sigma^*_{SiSi}$ excitation energy in Si–Si bonds compared with the $\sigma_{CC} - \sigma^*_{CC}$ excitation energy in C–C bonds.[4] Polysilanes typically absorb in the range 250–350 nm and the absorption is greatly influenced by the side groups attached to the silicon atoms. Previous reports have shown that the presence of aromatic groups on the silicon atoms cause a red shift of 25–35 nm in the UV absorption spectra and enhance σ–π mixing thereby increasing the conjugation across the system.[5] Organosilanes have a number of applications in both medicinal chemistry[6–8] and as energy materials.[9] The photoluminescent properties of silicon based materials have provided a new platform for polysilanes to act as chemo sensors for detecting explosive materials such as 2,4,6-trinitrotoluene (TNT) and picric acid.[10–12] Being photoactive in nature, long chain organosilanes have also been tested for photoconductivity and photocurrent generation.[13–15]

Despite having the potential to be used in various applications, the Si–Si sigma bonds cleave upon excessive exposure to UV radiation, therefore limiting the applications of these materials.[5] For example, successive blue shifts were observed in the UV spectra of oligosilanes over time indicating photodecomposition.[16] Sakurai *et al.* proposed a radical mechanism for the photodecomposition of the Si–Si bonds as they successfully isolated the silyl radicals, as detected by electron paramagnetic resonance spectroscopy, for an aryldisilane in cyclohexane.[17]

We propose that reinforcing the Si–Si bond in a disilane, using a tether in the form of a covalent bridge, is a potential way to support the weak Si–Si bonds. In the presence of a bridge, upon UV irradiation, the silyl radicals formed during photodecomposition will remain in close proximity to each other, therefore creating a greater chance for the two silyl radicals to recombine, reforming the covalent Si–Si bond. The bridge could be either alkyl or aromatic. Since aromatic groups attached to the silicon atoms leads to σ–π mixing, attaching aromatic substituents will presumably enhance the semi-conducting properties of the material owing to increased conjugation. Evidence for this was observed in studies conducted by Klausen *et al.*[18] wherein the conductivity of the disilanes containing sulfur tethers were measured by a scanning tunnelling microscope (STM) break junction technique.

In our quest to prepare oligosilanes that are robust, with increased conjugation that can ultimately be used for opto-electronics, substituted naphthalene bridged disilanes seemed to be the best candidates. We have previously reported[19] that naphthalene disilanes increase the overall conjugation owing to the σ–π mixing and also benefit the geometry of the resulting five membered ring system as the Si–Si bond length matches with that of the 1,8-substitution of naphthalene. In this study, we investigated the effects of modifying the substitution around the silicon atoms in the naphthalene bridged disilanes on their photophysical properties in organic solvents of varying polarity. The three target bridged disilanes (**1b**, **2b** and **3b**, Fig. 1), two of which are structural isomers of each other, were prepared.

[a]*School of Chemical Sciences, The University of Auckland, Private Bag, 92019, Auckland, 1142, New Zealand. E-mail: erin.leitao@auckland.ac.nz*

[b]*The MacDiarmid Institute for Advanced Materials and Nanotechnology, New Zealand*

[c]*Centre for Biomedical and Chemical Sciences, School of Science, Auckland University of Technology, Private Bag 92006, Auckland 1142, New Zealand*

[d]*School of Chemical and Physical Sciences, Victoria University of Wellington, PO Box 6006140, New Zealand*

† Electronic supplementary information (ESI) available. CCDC 2060937 and 2060939. For ESI and crystallographic data in CIF or other electronic format see DOI: 10.1039/d1ra02961d

Results and discussion

The target naphthalene bridged disilane precursors **1a**, **2a** and **3a** (Scheme 1) were synthesised using previously reported methodologies (Fig. S1–S7†).[19–21] A two-step lithiation process to synthesize **1a** was used in order to introduce the two different silanes. 1,8-Dibromonapthalene was monolithiated with *n*-butyllithium and further reacted with a chlorodimethylsilane ($ClSiMe_2H$) to form **1**. After purification, **1** was further lithiated and reacted with chlorodiphenylsilane ($ClSiPh_2H$) to produce **1a** as a white solid. The disilyl naphthalene derivatives (**2a** and **3a**) were prepared from 1,8-dibromonapthalene, which was reacted with *n*-butyllithium to form 1,8-dilithiated naphthalene *in situ*. Followed by a slight excess of the respective chlorosilanes (*e.g.* PhMeSiClH or Me_2SiClH) the formation of the required chiral and tetramethyl substituted disilyl naphthalene derivatives, **2a** and **3a** respectively, were obtained.

The disilyl precursors (**1a**, **2a** and **3a**) were subjected to intramolecular dehydrocoupling using 5 mol% of $RhCl(PPh_3)_3$ in toluene to produce the asymmetric naphthalene bridged disilane **1b** (Fig. S8–S10†) and the symmetric naphthalene bridged disilane **2b** and **3b** (Scheme 2). Interestingly, it was observed that **1b** and **3b** existed as a crystalline solid, whereas, the chiral **2b** was obtained as a waxy substance. Product **1b** was dissolved in pentane and stored at −20 °C to grow single crystals (Fig. 2). However, repeated attempts to crystallise **2b**, such as freezing at −20 °C and −40 °C in pentane for 24 h and 2 h, respectively, did not yield any crystalline solids, leaving the waxy substance after removal of pentane.

The five membered ring in **1b** was observed to be slightly distorted from planarity. The C13–Si1–Si2 bond angle was 93.02° compared with the C21–Si2–Si1 bond angle of 91.86° indicating the effect of steric bulk on the two silicon centres (Table S1†). The bond angles around the silicon centre bearing the bulkier phenyl rings were narrower compared with the silicon centre containing methyl groups. The Si1–Si2 bond distance was 2.33 Å which was similar to the **3b** derivative.[19] NMR spectroscopy and GC-MS analysis of **2b** (Fig. S11–S15†) confirmed that the product obtained was a mixture of two isomers. The *cis* and *trans* isomers of the product **2b** could not be separated by silica gel column chromatography or high-pressure flash chromatography as the mixture showed no separation on TLC despite varying the solvent polarities.

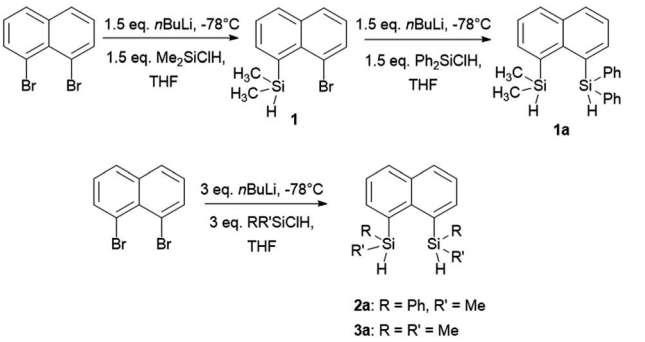

Scheme 1 Synthesis of disilyl precursors **1a**, **2a** and **3a**.

For the studies of the photophysical properties, naphthalene was selected as the parent compound. Absorption and emission spectra of naphthalene and the three-bridged disilanes (**1b**, **2b** and **3b**) were obtained in organic solvent of varying polarity (Table 1 and Fig. S17–S20†). In comparison to naphthalene, the absorption spectra of the bridged disilanes **1b**, **2b** and **3b** displayed red-shifted absorption, thereby indicating the extended conjugation in the bridged systems. The absorption maxima of the naphthalene and compounds **1b–3b** showed very little dependency on solvent polarity. The emission profiles were recorded in the same set of solvents (Fig. 3) at an excitation wavelength of 305 nm for **1b**, **2b** and **3b** and 286 nm for naphthalene. In THF and acetonitrile, the emission spectra of the bridged silanes (**1b**, **2b** and **3b**) exhibited vibronic fine structure (maxima at *ca.* 335 and 345 nm), displaying a close resemblance to that of naphthalene. However, upon moving to non-polar solvents (cyclohexane and toluene), an additional broad emission band at longer wavelengths (>400 nm) is observed, suggesting the formation of excimers (excited state dimers, Fig. 3). The presence of this additional emission band in non-polar solvents was not observed for naphthalene.

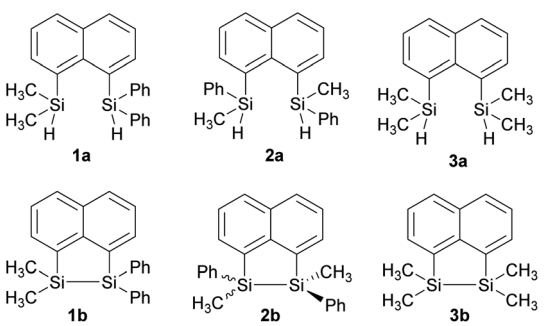

Fig. 1 Substituted disilyl naphthalene precursors (**1a**, **2a** and **3a**) and naphthalene bridged disilanes (**1b**, **2b**, and **3b**).

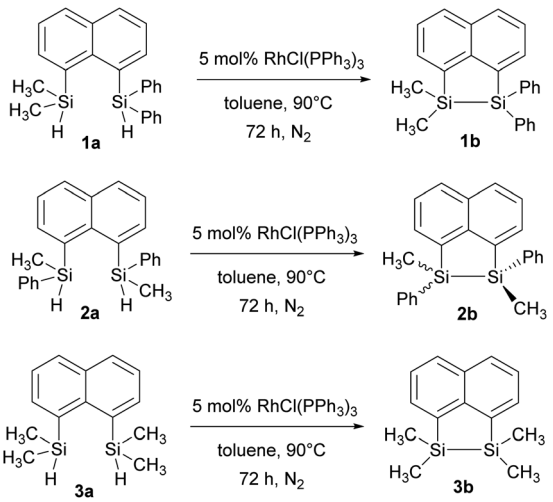

Scheme 2 Intramolecular dehydrocoupling of **1a**, **2a** and **3a** to produce the bridged disilanes **1b**, **2b** and **3b**.

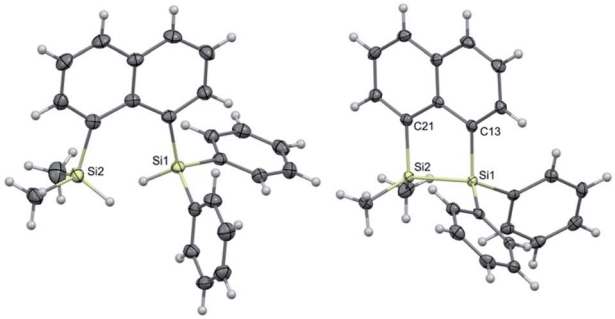

Fig. 2 Molecular structures of **1a** (left) and **1b** (right, only one of the two crystallographically independent molecules is shown) with thermal ellipsoids shown at 50% probability level.

Excimers form between identical molecules, when a monomer in the excited state interacts with another monomer in the ground state, which subsequently relaxes by dissociation and involves emission of photons.[22] Concentration studies were conducted in cyclohexane (Fig. 4) and THF (Fig. S21–S24†) to provide further evidence for the presence of excimers in non-polar solutions. As excimers are favoured at higher concentrations, it was anticipated that the broad band observed at >400 nm in cyclohexane would decrease upon dilution. As illustrated in Fig. 4(ii), the emission spectrum of compound **1b** in cyclohexane is highly dependent on concentration. Upon dilution of a 2.54×10^{-4} M solution of **1b**, the broad emission band at 407 nm significantly decreases. The same trend was also observed for compounds **2b** and **3b** (Fig. 4(iii and iv)). In contrast, the emission spectrum of naphthalene in cyclohexane at varying concentrations remained unchanged (Fig. 4(i)).

Measurements of the photoluminescence quantum yields of the naphthalene bridged disilanes (**1b**, **2b** and **3b**) corroborated these results (Table 1). In THF, the three derivatives exhibit weak to moderate fluorescence (compounds **1b** and **3b** φ_F <0.01; compound **2b** $\varphi_F = 0.09$). However, in non-polar solvents (cyclohexane and toluene) all three compounds show an increase in fluorescence quantum yields ($\varphi_F = 0.15$–0.32) due to the formation of excited state dimers. Interestingly, for **2b**, a high fluorescence quantum yield in acetonitrile ($\varphi_F = 0.49$) is also observed.

Several literature examples of excimer formation in molecules containing a naphthalene moiety have been reported.[22–25] Pandeeswer *et al.* and Boer *et al.* observed broad peaks in the visible regions for naphthalene diimides in polar as well as non-polar solvents.[22,25] Similarly, L'Her *et al.* observed broad peaks in the visible regions for imidazolium-naphthalene salts in DCM.[23] However, to the best of our knowledge, this is the first example where excimers are observed through intermolecular interactions between naphthalene in bridged disilane compounds. It is also important to note that this phenomenon was not observed in the disilyl naphthalene precursors, prior to the formation of the Si–Si bond. This was evident from the detailed photophysical study conducted by Maeda *et al.* on various silyl naphthalene compounds, similar to **1a–3a** in non-polar solvents.[26] As such, it appears that the Si–Si bond plays a key role in the formation of excimers in the compounds **1b–3b**. The work of Karatsu *et al.* also highlighted the significance the presence of the Si–Si bond has on excimer formation.[27–30] In their investigation, the photophysical properties of a series of permethyloligosilanes of varying length ($[Me_2Si]_n$, $n = 1$–4, 6), containing naphthalene or anthracene groups on the terminal silicon atoms, were explored. The two aromatic groups on the ends of the oligosilane chains have the ability interact *via* π-stacking, forming an *intramolecular* sandwich. In cases where the number of silicon atoms in the chain was greater than 1, intramolecular excimer formation

Table 1 Spectroscopic data for naphthalene and compounds **1b**, **2b**, **3b**[a]

Compound	Solvent	λ_{abs}[b] (nm)	ε_{max} (M^{-1} cm^{-1})	λ_{em}[c] (nm)	Φ_F[d]
Naphthalene	Cyclohexane	276	5976	324	nd
	Toluene	nd	nd	nd	nd
	THF	276	4499	323	nd
	ACN	274	nd	322	nd
1b	Cyclohexane	292	4230	407	0.17
	Toluene	293	nd	427	0.17
	THF	293	9017	335	0.007
	ACN	292	nd	336	0.05
2b	Cyclohexane	292	6797	335, 413[e]	0.19
	Toluene	293	nd	335, 427[f]	0.15
	THF	292	7097	336	0.09
	ACN	292	nd	335	0.49
3b	Cyclohexane	290	10 635	376	0.20
	Toluene	289	nd	405	0.32
	THF	291	8345	335	0.008
	ACN	290	nd	335	0.13

[a] nd = not determined. [b] Wavelength of the absorption maximum. [c] Wavelength of the emission maximum; for naphthalene, excitation wavelength was 286 nm. For compounds **1b–3b**, excitation wavelength was 305 nm. [d] Fluorescence quantum yield for compounds **1b–3b** in different solvent, excitation wavelength range 285–295 nm. [e] Emission band ascribed to the formation of excimers. [f] Emission band ascribed to the formation of excimers. Naphthalene was not measured in toluene due to the strong absorption of toluene in the UV region in which naphthalene absorbs.

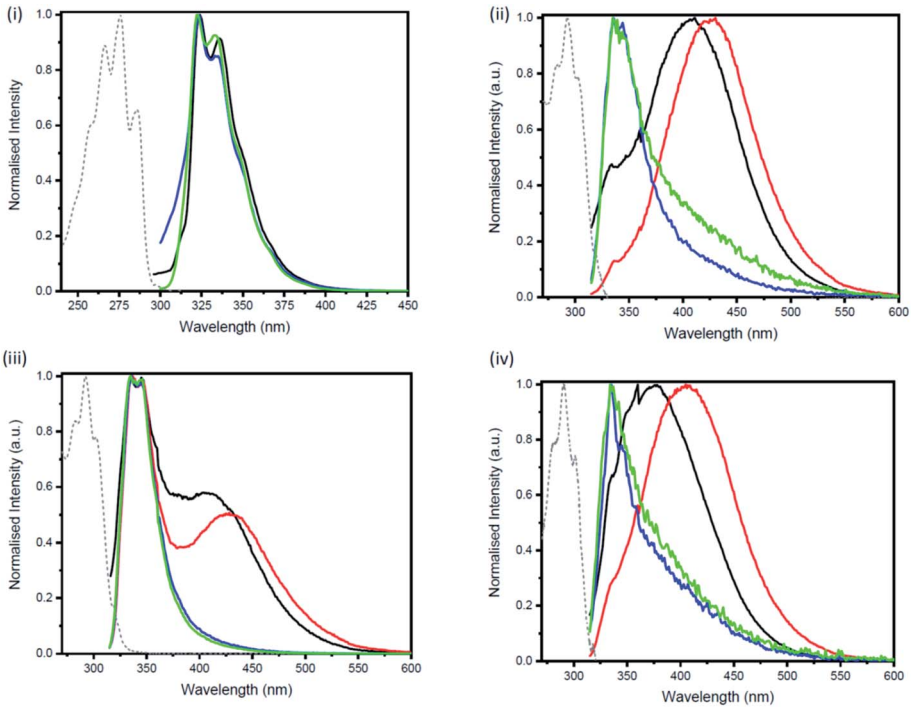

Fig. 3 Absorption (dashed) and emission (solid) profiles of (i) naphthalene, (ii) **1b**, (iii) **2b**, and (iv) **3b** in cyclohexane (*black*), toluene (*red*), THF (*blue*), acetonitrile (*green*). Absorption spectrum is that recorded in THF.

was observed in cyclohexane. Interestingly, when the oligosilane chain was tetramethyl disilane ($n = 2$), the strongest excimer fluorescence was observed,[27] indicating the disilane tether provides the optimal distance between the two end groups (*i.e.* naphthalene or anthracene). Furthermore, unlike in our study, excimer formation occurred for the shorter chain oligomers ($n = 2$, 3 for naphthalene and $n = 2$–4 for anthracene) in polar solvent (*e.g.* acetonitrile) as well.

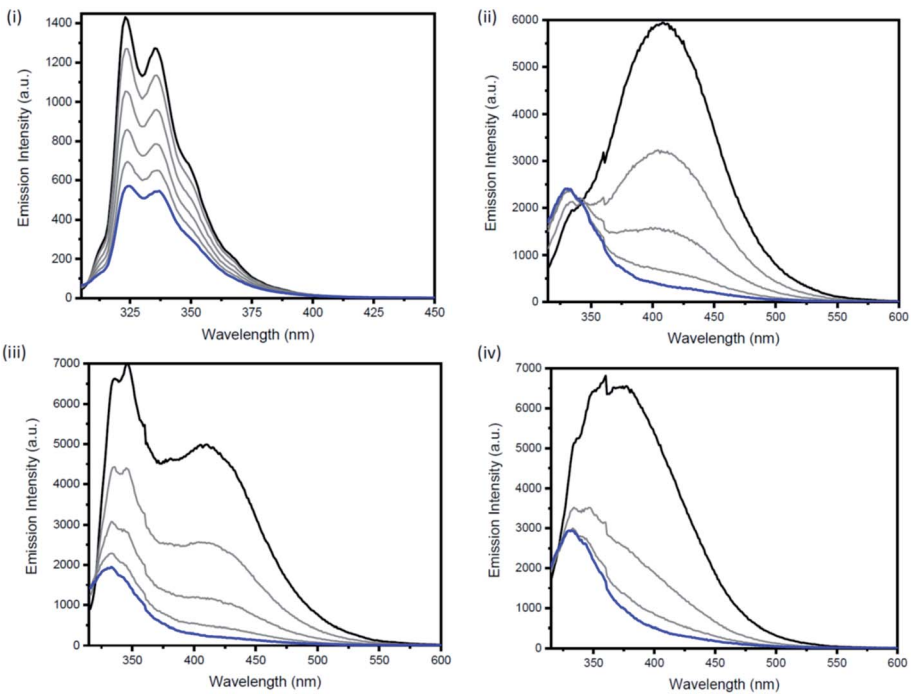

Fig. 4 Concentration dependent emission of (i) naphthalene upon excitation at 286 nm (1.76×10^{-4} M (*black*) → 2.33×10^{-5} M (*blue*)), (ii) **1b** upon excitation at 305 nm (2.54×10^{-4} M (*black*) → 3.10×10^{-6} M (*blue*)), (iii) **2b** upon excitation at 305 nm (1.36×10^{-4} M (*black*) → 1.61×10^{-6} M (*blue*)) and (iv) **3b** upon excitation at 305 nm (3.20×10^{-5} M (*black*) → 1.20×10^{-6} M (*blue*)) in cyclohexane.

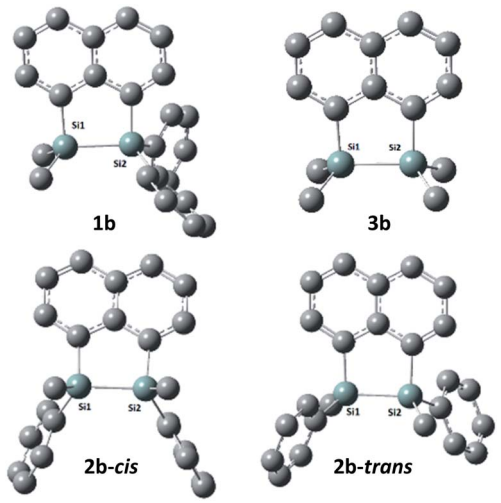

Fig. 5 Optimized geometries of **1b**, **2b(cis/trans)** and **3b**. (Hydrogen atoms are omitted for clarity).

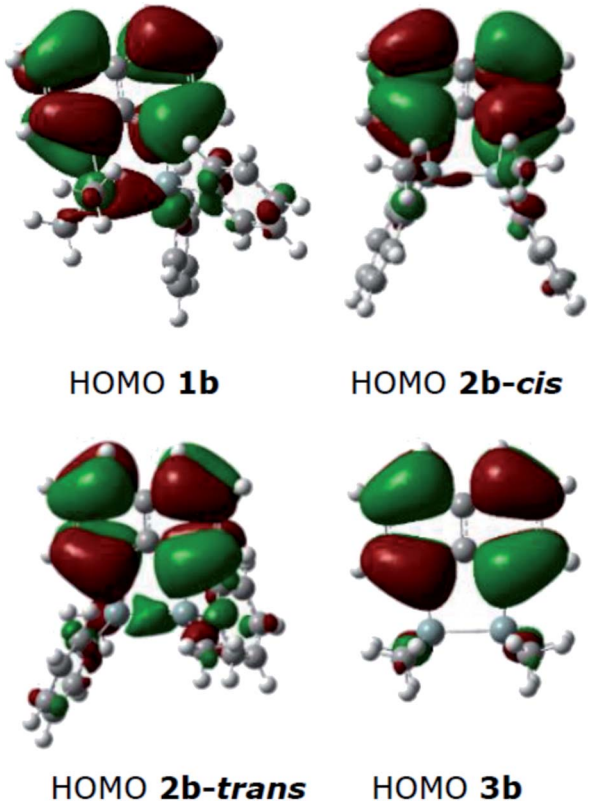

Fig. 6 HOMO diagrams from the optimised structures of **1b**, **2b**(*cis*/*trans*) and **3b**.

The electrochemical behaviour of the bridged disilanes (**1b**, **2b**, **3b**) was determined using cyclic voltammetry (CV) in dry acetonitrile under inert atmosphere with ferrocene as an internal standard to calibrate the potentials (Fig. S25–S27†). The electrochemical oxidation (E_{ox}) and reduction (E_{red}) potentials were used to calculate the HOMO–LUMO band gaps of the three bridged disilanes relative to ferrocene/ferrocenium (4.8 eV below the vacuum level).[31,32] The band gaps for **1b** and **2b** were found to be similar (3.62 eV and 3.67 eV, respectively) and lower than the calculated value for compound **3b** (3.85 eV) (Table S2†). This was expected due to the extra π-conjugation afforded by the phenyl substituents in compounds **1b** and **2b**.

DFT calculations were performed using Gaussian 09 software package,[33] for **1b**, the two isomers of **2b** (**2b-*cis*** and **2b-*trans***, Fig. 5), **3b** and naphthalene to calculate their band gaps in the gas phase and in solution phases using B3LYP/6-31++G**. The band gaps of **1b** and **2b** isomers varied form 4.01 eV to 4.07 eV and were lower in value than **3b** and naphthalene (Table 2) similar to the trend observed by the CV experiments. The lower relative band gaps for compounds **1b** and **2b** can be attributed to the presence of phenyl substituents on each silicon atom, increasing the overall conjugation. The diagrams depicting the HOMO of the same set of compounds (Fig. 6) indicated that the naphthalene also extended the overall conjugation of the system. This extended conjugation, a result of the σ–π mixing responsible for the reduction in the band gaps, is well established in the literature.[34] Another way to lower the band gap is to increase the number of Si atoms in the chain.[16] It was observed that the electronic contribution from the naphthalene rings was significantly more substantial than the phenyl rings attached to the Si centres, and that all the aromatic rings contributed to the σ–π mixing therefore explaining the difference in the band gap values between the various bridged silanes (**1b** and **2b**) and **3b**. Similar results were obtained for the other naphthalene based bridged systems recently reported by our group.[19]

Table 2 Calculated band gaps of **1b**, **2b-*cis***, **2b-*trans*** and **3b** in both gas and solution phases by TD-SCF(DFT).[35]

	Gas phase		THF		Cyclohexane	
Compound	Band gap (eV)	λ_{max} (nm)	Band gap (eV)	λ_{max} (nm)	Band gap (eV)	λ_{max} (nm)
1b	4.06	305.0	4.02	308.0	4.02	308.0
2b-*cis*	4.07	304.2	4.05	306.0	4.05	306.0
2b-*trans*	4.04	306.4	4.01	308.5	4.02	308.0
3b	4.14	299.0	4.10	302.0	4.10	302.0
Naphthalene	4.32	286.5	4.29	289.0	4.28	289.4

Conclusions

A series of naphthalene bridged disilanes (**1b**, **2b**, **3b**) containing different arrangements of methyl and phenyl substituents at silicon were synthesised, characterised and the photophysical properties were investigated. Experimental results and DFT calculations suggested that the Si–Si bonds as well as the presence of aromatic groups, particularly naphthalene, attached to the Si atoms contributed to the lowering of the band gaps. For example, λ_{max} was higher for **1b** and **2b** than **3b**. Furthermore, interchanging the substitution on the silicon atoms in the disilane derivatives resulted in significant changes in the photophysical properties that were observed. The naphthalene disilane derivatives **1b** (asymmetric with $SiMe_2$ and $SiPh_2$ substitution) and **3b** (no Ph substituents) both absorbed in the UV region and showed weak emission in the near-UV region, similar to naphthalene. In contrast, the symmetric, naphthalene disilane mixture **2b(*cis*/*trans*)** showed an intense emission peak in polar solvents. On switching to non-polar solvents such as cyclohexane and toluene, broadening in the visible region, corresponding to the presence of excimers, was observed in the emission profile for all three disilane molecules. As expected, concentration studies performed showed that a decrease in the concentration led to a decrease in the broad band at *ca*. 430 nm. The photoluminescence observed for **2b** presents opportunities to use this compound in applications such as light emitting devices or as a photocurrent generator in solar cells. Further derivatising these molecules as well as studying their potential in applications is ongoing in our laboratory.

Experimental

General information

All the experiments and manipulations were performed under nitrogen atmosphere in an MBraun Unilab 1200/780 glovebox or using conventional Schlenk techniques. All glassware was oven-dried overnight in a 135 °C oven. 1,8-Dibromonaphthalene and Wilkinson's catalyst were purchased from AK Scientific, chlorodimethylsilane and chlorodiphenylsilane were purchased from Sigma-Aldrich, chloromethylphenylsilane was purchased from Gelest. Materials were used directly as received. Ether and toluene were obtained from solvent purification system and later dried over activated molecular sieves (3 Å).

Instrumentation

^1H, ^{13}C and $^{29}Si\{^1H\}$ DEPT NMR, ^1H–^{29}Si HSQC NMR spectra were recorded on Bruker DPX-400 (400 MHz) spectrometer. Chemical shifts were reported in parts per million (ppm) relative to tetramethylsilane and are referenced to residual protium in the NMR solvent (*e.g.*, $CHCl_3$ = 7.26 ppm) as the internal standard. The silicon NMR resonances were determined with a DEPT pulse sequence. Data are represented as follows: chemical shift (δ), multiplicity (s = singlet, d = doublet, t = triplet, q = quartet, p = quintet, sep = septet, m = multiplet), coupling constants in Hertz (Hz) and integration. High resolution mass spectrometry measurements were made on a Bruker microTOF-QII mass spectrometer, equipped with a KD Scientific syringe pump, in positive ion ESI mode. Hard ionization mass spectrometry analysis was performed on Agilent 7890A GC + 5975C EI-MS with Agilent auto-sampler. X-ray diffraction analysis of single crystals of **1a** and **1b** were performed on a Rigaku Oxford Diffraction XtaLAB-Synergy-S single crystal diffractometer with a PILATUS 200 K hybrid pixel array detector using Cu Kα radiation (λ = 1.54184 Å; ESI Table 1†). The data was processed with the SHELX2018/3 and Olex2 1.3 software packages.[36,37] All non-hydrogen atoms were refined anisotropically. Hydrogen atoms were inserted at calculated positions and refined with a riding model or located in the difference Fourier map and refined without restrictions (silane hydrogen atoms). Mercury 2020.3.1 was used to visualize the molecular structures.[38] UV-Vis spectra were recorded on a Shimadzu UV-3600 Plus spectrophotometer and the fluorescence emission spectra were recorded on a Jasco FP-8600 spectrofluorometer. Samples were recorded in a macro quartz cuvette (light path = 10 × 10 mm). Fluorescence quantum yields were determined using an Edinburgh Photonics FLS-980 spectrophotometer equipped with an integrating sphere, using a 450 W ozone free xenon arc lamp as the light source. CV experiments were performed using a BAS CGME controlled mercury stand cell. All the DFT calculations were performed using Gaussian 09.[33] The geometries of all the subject molecules were optimised using the B3LYP functional and 6-311++G** basis set.[39–41]

Preparation of 1a

1a was synthesized *via* a literature procedure and the NMR data was in excellent agreement with the published compound.[21]

Preparation of 2a

To a 100 mL Schlenk flask equipped with a stir bar was added 1,8-dibromonaphthalene (2 mmol, 0.571 g) and 15 mL THF solvent. The solution was cooled to −78 °C using a dry ice-acetone bath, to which was added *n*-BuLi (2.0 M in cyclohexane, 3.0 equiv., 6 mmol, 3 mL) dropwise and the mixture was stirred at −78 °C for 1 hour. To the lithiated mixture was added chloromethylphenylsilane (3 equiv., 6 mmol, 0.9 mL) and was stirred at 22 °C overnight. The reaction mixture was quenched with saturated solution of $NaHCO_3$ (5 mL) and the aqueous layer was extracted with diethyl ether (3 × 10 mL). All the organic layers were combined and dried over Na_2SO_4. The crude product was obtained upon removal of solvents under vacuum as a yellow gummy substance. The crude was purified over silica gel column, using 100% hexanes as the eluent, to obtain non-separable diastereomers of **2a** as a blueish-yellow gum in 64.3% yield.

^1H NMR (400 MHz, $CDCl_3$): δ 7.92–7.26 (m, Ph, 16H), 5.59 (*p*, SiH, 2H), 0.69 (dd, CH_3, 6H). $^{13}C\{^1H\}$ NMR (100.6 MHz, $CDCl_3$): δ 144.19, 139.80, 139.68, 139.59, 137.46, 137.42, 137.05, 137.00, 135.88, 133.66, 131.10, 129.85, 129.79, 126.53, −0.08. $^{29}Si\{^1H\}$ NMR (79.5 MHz, $CDCl_3$): δ −20.37. EI: Found for $C_{24}H_{24}Si_2$: 368.19 *m*/*z*, calc'd: 368.14 *m*/*z*.

Preparation of 1b

To a 50 mL Schlenk flask was added **1a** (1 mmol, 0.37 g), Wilkinson's catalyst (5 mol%, 0.05 mmol, 46 mg) and 10 mL toluene. The mixture was heated at 90 °C for 72 hours. To the mixture was added 15 mL hexanes and the mixture was filtered through a Florisil column. The colorless solution was concentrated under high vacuum to remove the solvents and obtain the crude product. The crude was re-dissolved in pentane (7 mL) and was stored at −20 °C overnight to obtain colorless crystals of **1b** in 30.0% yield.

^{1}H NMR (400 MHz, $CDCl_3$): δ 8.02–7.38 (m, Ph, 16H), 0.56 (s, CH_3, 6H). $^{13}C\{^{1}H\}$ NMR (100.6 MHz, $CDCl_3$): δ 141.86, 134.8, 133.47, 133.11, 131.78, 130.89, 128.62, 128.16, 126.94, 124.94, 124.90, −3.54. $^{29}Si\{^{1}H\}$ NMR (79.5 MHz, $CDCl_3$): δ −20.62. EI: found for $C_{24}H_{22}Si_2$: 366.14 *m*/*z*, calc'd: 366.12 *m*/*z*.

Preparation of 2b

To a 50 mL Schlenk flask was added **2a** (1.2 mmol, 0.47 g), Wilkinson's catalyst (5 mol%, 0.06 mmol, 55 mg) and 10 mL toluene. The mixture was heated at 90 °C for 72 hours. To the mixture was added 15 mL hexane and the mixture was filtered through a Florisil column. The colorless solution was dried under high vacuum to obtain the crude product. The crude was washed with cold pentane (2 × 5 mL) to obtain pure **2b** as blueish-yellow gum in 24.5% yield.

From the proton NMR spectrum, it was evident that the product was a mixture of *cis* and *trans* isomers in 2 : 1 ratio respectively. Similar results were observed by Kim *et al.*,[42] and based on their findings, it is concluded that the *cis* isomer was present in higher amount than the *trans* isomer.

^{1}H NMR (400 MHz, $CDCl_3$): δ 7.90–7.10 (m, Ph, 24H), 0.75 (s, *cis*-CH_3, 6H), 0.60 (s, *trans*-CH_3, 3H). $^{13}C\{^{1}H\}$ NMR (100.6 MHz, $CDCl_3$): δ 145.70, 140.09, 140.03, 135.47, 133.87, 133.70, 133.02, 132.09, 131.71, 129.83, 128.70, 128.40, 127.87, 126.87, 126.87, 126.61, 125.00, 123.89, −5.71, −6.09. $^{29}Si\{^{1}H\}$ NMR (79.5 MHz, $CDCl_3$): δ −22.90, −23.33. EI: found for $C_{24}H_{22}Si_2$: 366.12 *m*/*z*. calc'd: 366.16 *m*/*z*.

Preparation of 3a and 3b

3a and **3b** were synthesized *via* a literature procedure and the NMR data was in good agreement with what was reported.[19]

Conflicts of interest

There are no conflicts to declare.

Acknowledgements

The authors would like to acknowledge the support provided by the School of Chemical Sciences, University of Auckland and the MacDiarmid Institute. VBK, SM, PAH, and EML thank Royal Society of New Zealand Marsden Fast-Start grant for the financial support and doctoral scholarships for VBK and SM. NJLKD acknowledges research funding from the Victoria Research Trust, the Science for Technological Innovation Science Challenges, the Marsden Fund, the Ministry of Business, Innovation and Employment and the Royal Society of New Zealand. We thank Tatiana Grousto for collecting the single crystal X-ray diffraction data and Dr David Ware and David Goodman for their assistance with the CV measurements. The theoretical studies were enabled by the services provide by New Zealand e-Science Infrastructure (NeSI).

Notes and references

1 R. West, L. D. David, P. I. Djurovich, K. L. Stearley, K. S. V. Srinivasan and H. Yu, *J. Am. Chem. Soc.*, 1981, **103**, 7352–7354.
2 E. Orti, R. Crespo, M. C. Piqueras, F. Tomas and J. L. Bredas, *Synth. Met.*, 1993, **57**, 4419–4424.
3 R. G. Kepler, *Synth. Met.*, 1989, **28**, 573–580.
4 J. Michl, *Acc. Chem. Res.*, 1990, **23**, 127–128.
5 R. D. Miller and J. Michl, *Chem. Rev.*, 1989, **89**, 1359–1410.
6 M. J. Barnes, R. Conroy, D. J. Miller, J. S. Mills, J. G. Montana, P. K. Pooni, G. A. Showell, L. M. Walsh and J. B. H. Warneck, *Bioorg. Med. Chem. Lett.*, 2007, **17**, 354–357.
7 A. K. Franz and S. O. Wilson, *J. Med. Chem.*, 2013, **56**, 388–405.
8 S. M. Sieburth, T. Nittoli, A. M. Mutahi and L. Guo, *Angew. Chem., Int. Ed.*, 1998, **37**, 812–814.
9 V. B. Kumar and E. M. Leitao, *Appl. Organomet. Chem.*, 2020, **34**, e5402.
10 K. Amro, S. Clément, P. Déjardin, W. E. Douglas, P. Gerbier, J.-M. Janot and T. Thami, *J. Mater. Chem.*, 2010, **20**, 7100–7103.
11 S. J. Toal, D. Magde and W. C. Trogler, *Chem. Commun.*, 2005, 5465–5467.
12 W. Shu, C. Guan, W. Guo, C. Wang and Y. Shen, *J. Mater. Chem.*, 2012, **22**, 3075–3081.
13 Y. Nakayama, A. Saito, T. Fujii and S. Akita, *Photocarrier generation in polysilane films doped with and without fullerene*, 1999.
14 R. G. Kepler, J. Zeigler, L. A. Harrah and S. R. Kurtz, *Photocarrier generation and transport in -bonded polysilanes*, 1987.
15 A. O. Kawashima, T. Oku, A. Suzuki, K. Kikuchi and S. Kikuchi, *Mater. Sci. Appl.*, 2012, **3**, 557–561.
16 P. Trefonas Iii, R. West, R. D. Miller and D. Hofer, *J. Polym. Sci., Polym. Lett. Ed.*, 1983, **21**, 823–829.
17 H. Sakurai, Y. Nakadaira, M. Kira, H. Sugiyama, K. Yoshida and T. Takiguchi, *J. Organomet. Chem.*, 1980, **184**, C36–C40.
18 R. S. Klausen, J. R. Widawsky, M. L. Steigerwald, L. Venkataraman and C. Nuckolls, *J. Am. Chem. Soc.*, 2012, **134**, 4541–4544.
19 K. M. Rabanzo-Castillo, M. Hanif, T. Söhnel and E. M. Leitao, *Dalton Trans.*, 2019, **48**, 13971–13980.
20 W. Ando, T. Wakahara, T. Akasaka and S. Nagase, *Organometallics*, 1994, **13**, 4683–4685.
21 N. Lühmann, H. Hirao, S. Shaik and T. Müller, *Organometallics*, 2011, **30**, 4087–4096.
22 S. A. Boer, R. P. Cox, M. J. Beards, H. Wang, W. A. Donald, T. D. M. Bell and D. R. Turner, *Chem. Commun.*, 2019, **55**, 663–666.

23 M. L'Her, Y. Atoini, J. Fouchet, B. Heinrich, N. Del-Giudice, E. Scrafton, E. Bordes, L. Karmazin, L. Charbonière, L. De Cola and L. Douce, *New J. Chem.*, 2019, **43**, 12529–12532.
24 S. Asir, A. S. Demir and H. Icil, *Dyes Pigm.*, 2010, **84**, 1–13.
25 M. Pandeeswar and T. Govindaraju, *RSC Adv.*, 2013, **3**, 11459–11462.
26 H. Maeda, T. Maeda and K. Mizuno, *Molecules*, 2012, **17**, 5108–5125.
27 T. Karatsu, T. Shibata, A. Nishigaki, A. Kitamura, Y. Hatanaka, Y. Nishimura, S.-i. Sato and I. Yamazaki, *J. Phys. Chem. B*, 2003, **107**, 12184–12191.
28 T. Karatsu, T. Nakamura, M. Terasawa, S. Yagai, A. Kitamura, Y. Nishimura and I. Yamazaki, *Res. Chem. Intermed.*, 2013, **39**, 347–357.
29 T. Karatsu, T. Shibata, A. Nishigaki, K. Fukui and A. Kitamura, *Chem. Lett.*, 2001, **30**, 994–995.
30 T. Karatsu, *J. Photochem. Photobiol., C*, 2008, **9**, 111–137.
31 M. Shimada, Y. Yamanoi, T. Ohto, S.-T. Pham, R. Yamada, H. Tada, K. Omoto, S. Tashiro, M. Shionoya, M. Hattori, K. Jimura, S. Hayashi, H. Koike, M. Iwamura, K. Nozaki and H. Nishihara, *J. Am. Chem. Soc.*, 2017, **139**, 11214–11221.
32 T. Usuki, M. Shimada, Y. Yamanoi, T. Ohto, H. Tada, H. Kasai, E. Nishibori and H. Nishihara, *ACS Appl. Mater. Interfaces*, 2018, **10**, 12164–12172.
33 G. W. T. M. J. Frisch, H. B. Schlegel, G. E. Scuseria, J. R. C. M. A. Robb, G. Scalmani, V. Barone, G. A. P. B. Mennucci, H. Nakatsuji, M. Caricato, H. P. H. X. Li, A. F. Izmaylov, J. Bloino, G. Zheng, M. H. J. L. Sonnenberg, M. Ehara, K. Toyota, R. Fukuda, M. I. J. Hasegawa, T. Nakajima, Y. Honda, O. Kitao, T. V. H. Nakai, J. A. Montgomery Jr, J. E. Peralta, M. B. F. Ogliaro, J. J. Heyd, E. Brothers, K. N. Kudin, R. K. V. N. Staroverov, J. Normand, K. Raghavachari, J. C. B. A. Rendell, S. S. Iyengar, J. Tomasi, M. Cossi, J. M. M. N. Rega, M. Klene, J. E. Knox, J. B. Cross, C. A. V. Bakken, J. Jaramillo, R. Gomperts, O. Y. E. Stratmann, A. J. Austin, R. Cammi, C. Pomelli, R. L. M. J. W. Ochterski, K. Morokuma, G. A. V. V. G. Zakrzewskil, P. Salvador, J. J. Dannenberg, A. D. D. S. Dapprich, Ö. Farkas, J. B. Foresman and J. C. a. D. J. F. J. V. Ortiz, *Gaussian 09 Rev. D.01*, Wallingford, CT, 2013.
34 K. Takeda, H. Teramae and N. Matsumoto, *J. Am. Chem. Soc.*, 1986, **108**, 8186–8190.
35 J.-L. Bredas, *Mater. Horiz.*, 2014, **1**, 17–19.
36 O. V. Dolomanov, L. J. Bourhis, R. J. Gildea, J. A. K. Howard and H. Puschmann, *J. Appl. Crystallogr.*, 2009, **42**, 339–341.
37 G. Sheldrick, *Acta Crystallogr., Sect. A: Found. Adv.*, 2015, **71**, 3–8.
38 C. F. Macrae, P. R. Edgington, P. McCabe, E. Pidcock, G. P. Shields, R. Taylor, M. Towler and J. van de Streek, *J. Appl. Crystallogr.*, 2006, **39**, 453–457.
39 A. D. Becke, *Phys. Rev. A*, 1988, **38**, 3098–3100.
40 C. Lee, W. Yang and R. G. Parr, *Phys. Rev. B: Condens. Matter Mater. Phys.*, 1988, **37**, 785–789.
41 A. D. Becke, *J. Chem. Phys.*, 1993, **98**, 1372–1377.
42 N. T. Kim, H. Li, L. Venkataraman and J. L. Leighton, *J. Am. Chem. Soc.*, 2016, **138**, 11505–11508.